REGULAR ARTICLE

blood advances

Inverse relationship between oligoclonal expanded CD69$^-$ T_{TE} and CD69$^+$ T_{TE} cells in bone marrow of multiple myeloma patients

Slavica Vuckovic,[1-3,*] Christian E. Bryant,[1,4,*] Ka Hei Aleks Lau,[5] Shihong Yang,[4] James Favaloro,[1] Helen M. McGuire,[6-8] Georgina Clark,[3] Barbara Fazekas de St. Groth,[6-8] Felix Marsh-Wakefield,[7-9] Najah Nassif,[5] Edward Abadir,[1,4] Vinay Vanguru,[4] Derek McCulloch,[1,4,10] Christina Brown,[1,4,10] Stephen Larsen,[1,4,10] Scott Dunkley,[1,4] Liane Khoo,[1,4] John Gibson,[1,4,10] Richard Boyle,[11] Douglas Joshua,[1,10] and P. Joy Ho[1,4,10]

[1]Institute of Haematology, NSW Health Pathology, Royal Prince Alfred Hospital, Camperdown, NSW, Australia; [2]Faculty of Medicine, University of Queensland, St Lucia, QLD, Australia; [3]ANZAC Research Institute, Concord Repatriation General Hospital, Concord, NSW, Australia; [4]Institute of Haematology, Sydney Local Health District, Royal Prince Alfred Hospital, Camperdown, NSW, Australia; [5]School of Life Sciences, University of Technology Sydney, Ultimo, NSW, Australia; [6]Ramaciotti Facility for Human Systems Biology, The University of Sydney, Sydney, NSW, Australia; [7]Discipline of Pathology, Sydney Medical School, [8]Charles Perkins Centre, [9]Faculty of Medicine and Health, and [10]Sydney Medical School, The University of Sydney, Sydney, NSW, Australia; and [11]Orthopaedics Department, Royal Prince Alfred Hospital, Camperdown, NSW, Australia

Key Points

- Circulating cytotoxic CD69$^-$$T_{TE}$ cells mediating antimyeloma responses and noncytotoxic BM-resident CD69$^+$$T_{TE}$ cells exist in NDMM patients.
- A balance between CD69$^-$$T_{TE}$ and CD69$^+$ T_{TE} cells may regulate antimyeloma responses and contribute to clinical heterogeneity in NDMM patients.

CD8$^+$CD57$^+$ terminal effector T (T_{TE}) cells are a component of marrow-infiltrating lymphocytes and may contribute to the altered immune responses in multiple myeloma (MM) patients. We analyzed T_{TE} cells in the bone marrow (BM) and peripheral blood (PB) of age-matched controls and patients with monoclonal gammopathy of undetermined significance (MGUS), smoldering MM (SMM), and newly diagnosed (ND) MM using flow cytometry, mass cytometry, and FlowSOM clustering. T_{TE} cells are heterogeneous in all subjects, with BM containing both CD69$^-$ and CD69$^+$ subsets, while only CD69$^-$ cells are found in PB. Within the BM-T_{TE} compartment, CD69$^-$ and CD69$^+$ cells are found in comparable proportions in controls, while CD69$^-$ cells are dominant in MGUS and SMM and predominantly either CD69$^-$ or CD69$^+$ cells in NDMM. A positive relationship between CD69$^+$$T_{TE}$ and CD69$^-$$T_{TE}$ cells is observed in the BM of controls, lost in MGUS, and converted to an inverse relationship in NDMM. CD69$^-$$T_{TE}$ cells include multiple oligoclonal expansions of T-cell receptor/Vβ families shared between BM and PB of NDMM. Oligoclonal expanded CD69$^-$$T_{TE}$ cells from the PB include myeloma-reactive cells capable of killing autologous CD38^{hi} plasma cells in vitro, involving degranulation and high expression of perforin and granzyme. In contrast to CD69$^-$$T_{TE}$ cells, oligoclonal expansions are not evident within CD69$^+$$T_{TE}$ cells, which possess low perforin and granzyme expression and high inhibitory checkpoint expression and resemble T resident memory cells. Both CD69$^-$$T_{TE}$ and CD69$^+$$T_{TE}$ cells from the BM of NDMM produce large amounts of the inflammatory cytokines interferon-γ and tumor necrosis factor α. The balance between CD69$^-$ and CD69$^+$ cells within the BM-T_{TE} compartment may regulate immune responses in NDMM and contribute to the clinical heterogeneity of the disease.

Introduction

Multiple myeloma (MM) is a plasma cell (PC) neoplasm that is preceded by the premalignant condition monoclonal gammopathy of undetermined significance (MGUS) or asymptomatic, smoldering MM (SMM). In MM, malignant PCs in the bone marrow (BM) are accessible to T cells (marrow-infiltrating

Submitted 4 May 2020; accepted 24 August 2020; published online 28 September 2020. DOI 10.1182/bloodadvances.2020002237.

*S.V. and C.E.B. contributed equally to this study.

Data sharing statement: e-mails to the corresponding authors, Slavica Vuckovic (slavica.vuckovic@health.nsw.gov.au) and Christian E. Bryant (christian.bryant@health.nsw.gov.au).

The full-text version of this article contains a data supplement.

lymphocytes [MILs]) entering the BM by blood circulation. This proximity between PCs and T cells may facilitate autologous T-cell–mediated immune responses against malignant PCs. Direct evidence of autologous T-cell–mediated antimyeloma responses has been demonstrated in the Vk*MYC mouse model,[1,2] while a number of clinical studies provide indirect evidence to support autologous antimyeloma responses in humans.[3-6]

CD57 has been most widely explored as a marker of senescent $CD8^+$T cells.[7] Persistent immune stimulation is believed to induce the conversion of memory T (T_M) cells from $CD28^+CD57^-$ cells to senescent $CD28^-CD57^+$ cells characterized by limited proliferative capacity.[8] Acquisition of CD57 is thought to reflect a shift toward highly cytotoxic terminally differentiated effector T (T_{TE}) cells, with increased perforin and granzyme production.[9]

We have previously reported on the existence of oligoclonal expansions of T_{TE} cells, identified by expression of T-cell receptor (TCR) variable β (TCR-Vβ) families, in the peripheral blood (PB) of the majority of MM patients[7] and related their presence to a favorable prognosis.[10] Such oligoclonal expanded T_{TE} cells have lower expression of the inhibitory checkpoint CD279 (PD-1), suggesting that these cells may not be an optimal target for checkpoint blockade immunotherapy.[11,12] It has also been suggested that T_{TE} cells within MILs may impair immune responses to myeloma due to their senescent status.[13]

Expansion of oligoclonal T_{TE} cells in MM patients may result from persistent stimulation of $CD8^+$T cells by myeloma-associated antigens[6,14] in the absence of effective clearance of malignant clones. Recently, it has also been reported that progression from MGUS to MM involves attrition of the BM-resident T-cell compartment[15] and the appearance of exhausted T cells.[16] We considered that cytotoxic T_{TE} cells, being a constituent of MILs, may undergo changes that can help explain the altered immune responses observed in MM patients and provide novel ground for future immunotherapeutic approaches.[17]

In this study, we analyzed $CD8^+CD57^+T_{TE}$ cells in the BM and PB of age-matched controls and patients with MGUS, SMM, and newly diagnosed (ND) MM using fluorescence flow cytometry, mass cytometry,[18] and unsupervised FlowSOM clustering algorithm analyses.[19] We found that T_{TE} cells in all subjects can be subdivided by expression of CD69. $CD69^-T_{TE}$ cells circulate between PB and BM, while $CD69^+T_{TE}$ are restricted to the BM and have many characteristics in common with T resident memory (T_{RM}) cells. Within the BM-T_{TE} compartment, $CD69^-$ and $CD69^+$ cells are found in comparable proportions in controls, while $CD69^-$ cells are dominant in MGUS and SMM and predominantly either $CD69^-$ or $CD69^+$ cells in NDMM. Within the BM-T_{TE} compartment, a positive relationship between $CD69^+$ and $CD69^-$ cells is observed in controls, lost in MGUS, and converted to an inverse relationship in NDMM. We also demonstrated that the previously described oligoclonal expansions[7] are found within the $CD69^-T_{TE}$ cells in BM and PB, but not in $CD69^+T_{TE}$ cells, and that oligoclonal expanded cells from the PB of NDMM patients are capable of eliminating autologous $CD38^{hi}$PCs in vitro involving degranulation and high expression of perforin and granzyme B.

Materials and methods

Patients and controls

MGUS, SMM, and NDMM patients, diagnosed using the criteria established by the International Myeloma Working Group,[20] were recruited through the Department of Hematology, Royal Prince Alfred Hospital (RPAH). Age-matched controls included healthy blood donors and patients without diagnosed malignancy or active infection, undergoing hip arthroplasty at the Department of Orthopedic Surgery, RPAH. Patients and controls characteristics are shown in Table 1. Where possible, paired BM and PB samples were collected and, dependent on sample availability, analyzed by mass cytometry, fluorescence flow cytometry, or both. The study was approved by the institutional human ethics committee. All patients signed informed consent before sample collection in accordance with the amended Declaration of Helsinki.

Fluorescence flow cytometry analyses

Fluorescence flow cytometry samples comprised fresh whole-blood samples, cryopreserved BM mononuclear cells (MNCs), and PB MNCs isolated by Ficoll-Hypaque density gradient. To analyze cytokine production, BM MNCs were rested overnight, sorted into $CD3^+CD69^-$ and $CD3^+CD69^+$ cells (BDFACS Aria II, BD Biosciences), and stimulated with phorbol 12-myristate 13-acetate and ionomycin calcium salt (Sigma-Aldrich) for 4 hours with the addition of protein transport inhibitor cocktail (Thermo Fisher Scientific) for the last 3 hours of culture. Following stimulation, cells were labeled with monoclonal antibodies (mAbs) targeting surface antigens (supplemental Table 1), fixed and permeabilized (fixation/permeabilization buffer, BD Biosciences), and stained with mAbs specific to interferon-γ (IFN-γ) and tumor necrosis factor α (TNF-α) in Perm/Wash buffer (BD Biosciences).

TCR-Vβ usage was analyzed using the IOTest β Mark TCR-Vβ Repertoire Kit (Beckman Coulter Life Sciences). TCR-Vβ family–expressing populations within a patient's T_{TE} were determined to be oligoclonally expanded when the percentage of T_{TE} cells expressing that TCR-Vβ family was more than 3 standard deviations (SDs) higher than the mean frequency within the naive $CD8^+$T (T_N) compartment of healthy blood donors. The dominant oligoclonal expansion in each patient was defined as the one representing the largest percentage of PB T_{TE} cells.

To analyze the elimination of autologous $CD38^{hi}$PCs (target) by $CD69^-T_{TE}$ cells (effectors), 2 subsets of T_{TE} cells were flow-sorted from PB MNCs: those expressing the dominant TCR-Vβ family and the remainder expressing all other TCR-Vβ families. Sorted cells were stimulated for 12 to 14 hours by CD2/CD3/CD28-loaded anti-biotin MACSiBead (Miltenyi Biotec) before the addition to the target cells; CD3-depleted autologous BM MNCs (effector/target ratio of 1:2). To assess degranulation and associated IFN-γ expression, αCD107a and protein transport inhibitor cocktail were added at the beginning of cell culture. Following 1 to 2 hours of culture, cells were labeled with mAbs targeting surface markers (supplemental Table 1), fixed and permeabilized, and stained depending on the experiment with mAbs specific to cleaved caspase-3 AF488, rabbit immunoglobulin G AF488, or IFN-γ in Perm/Wash buffer.

Mass cytometry staining and data acquisition

BM MNCs and PB MNCs from MGUS (n = 4) and NDMM (n = 8) patients were analyzed by mass cytometry. Cells were stained with 1.25 μL cisplatin (Fluidigm) followed by quenching and washing with fluorescence-activated cell sorter buffer. Cells were initially incubated with an AF647-labeled CD160 (BD Biosciences) mAb, followed by a cocktail of metal-conjugated mAbs targeting surface

Table 1. General and clinical characteristics of patients and controls

	NDMM (n = 36)	SMM (n = 11)	MGUS (n = 24)	Controls (n = 26)
Age, median (range), y	69 (38-90)	73 (50-85)	64 (42-89)	60 (35-84)
Sex, male, n (%)	20 (55)	5 (45)	7 (29)	12 (46)
ISS stage,* n (%)				
ISS1	11 (34)	3 (37.5)	NA	NA
ISS2	10 (32)	3 (37.5)	NA	NA
ISS3	11 (36)	2 (25)	NA	NA
Isotype, n (%)				
IgG	21 (60)	NA	NA	NA
IgA	8 (23)	NA	NA	NA
Light chain	6 (17)	NA	NA	NA
Oligosecretory	1 (3)	NA	NA	NA
Cytogenetics, n (%)	33 (92)	NA	NA	NA
17p deletion	4 (12)	NA	NA	NA
−1p and/or +1q	13 (40)	NA	NA	NA
FISH,† n (%)	20 (55)	NA	NA	NA
t(4;14)	2 (11)	NA	NA	NA
t(14;16)	0 (0)	NA	NA	NA
LDH,‡ median (range), U/L	157 (89-407)	NA	NA	NA
Above normal, n (%)	5 (18)	NA	NA	NA

FISH, fluorescence in situ hybridization; IgA, immunoglobulin A; IgG, immunoglobulin G; ISS, International Staging System; LDH, lactate dehydrogenase; NA, not available.
*β2 microglobulin available for ISS grading in 32 out of 36 NDMM patients and 8 out of 11 SMM patients.
†High-risk genetics by FISH, including del17p, t(4;14), and t(14;16), were tested in 20 out of 36 NDMM patients.
‡Available in 28 out of 36 NDMM patients.

proteins (supplemental Table 2). Cells were subsequently fixed and permeabilized (Foxp3 fixation kit, Thermo Fisher Scientific) and stained with metal-conjugated mAbs targeting intracellular proteins (supplemental Table 2). Cell acquisition occurred at a rate of 200 to 400 cells per second using a CyTOF 2 Helios upgraded mass cytometer (Fluidigm, Charles Perkins Centre, University of Sydney, NSW, Australia).

Analysis of mass cytometry data

After exclusion of $CD3^-CD38^{hi}$PCs, $CD56^+$NK cells, and $CD19^+$ B cells, BM-T_{TE} and PB-T_{TE} cells in MGUS and NDMM were manually gated based on CD57 expression within the $CD8^+$T gate, imported into R studio (v1.2.1135), and analyzed using the CAPX (v0.3) script, which includes both the clustering algorithm FlowSOM[19] and dimensionality reduction algorithm t-distributed stochastic neighbor embedding (tSNE)[21] in a single script.[22] tSNE plots were generated using the same 15 antigens selected for FlowSOM, with the addition of 3 TCR-Vβ antigens (supplemental Table 2) to allow visualization of oligoclonal expanded $CD69^-T_{TE}$ cells expressing dominant TCR-Vβ family.

Statistical analysis

The nonparametric Mann-Whitney *U* test was used to compare 2 variables, and the Kruskal-Wallis and Friedman test with Dunn's multiple comparisons was used to compare multiple unpaired and paired data sets, respectively. Relationships between 2 variables were analyzed by linear regression and between multiple variable by nonparametric Spearman correlation. Statistical significance was determined at Spearman $R < -0.5$ and > 0.5 and $P < .05$ for all statistical analyses using GraphPad Prism version 8.02 (GraphPad Software).

Results

T_{TE} cells within BM and PB of controls and MGUS, SMM, and NDMM patients

We initially characterized $CD8^+CD57^+T_{TE}$ cells in the BM and PB of age-matched controls and patients with MGUS, SMM, and NDMM by fluorescence flow cytometry. In all subjects, BM-T_{TE} cells contained both $CD69^-$ and $CD69^+$ subsets, whereas PB T_{TE} cells contained only the $CD69^-$ cell subset (Figure 1). Although $CD69^+$ T_{TE} cells were "resident" within BM, only a minority expressed another marker of residency, CD103[23] (supplemental Figure 1). $CD69^-$ and $CD69^+$ cells accounted for comparable proportions of BM-T_{TE} cells in controls, while $CD69^-$ cells dominated within BM-T_{TE} cells of MGUS and SMM patients (Figure 1B). Neither of these trends was apparent in BM-T_{TE} cells of NDMM patients; instead, $CD69^-$ cells in some patients and $CD69^+$ cells in other patients represented the majority of BM-T_{TE} compartment (Figure 1B). In addition, $CD69^-$ and $CD69^+$ subsets, as well as total BM-T_{TE} cells, accounted for highly variable proportions of BM-$CD8^+$T cells in NDMM (Figure 1C; supplemental Figure 2A). Despite interpatient variability, $CD69^-T_{TE}$ and total T_{TE} cells were significantly increased in the BM of NDMM patients compared with controls (expressed as a percentage of $CD8^+$T cells; Figure 1C; supplemental Figure 2A). In contrast to BM T_{TE} cells, PB $CD69^-T_{TE}$ and total PB T_{TE} cells were present in similar proportions in all subjects (Figure 1B-C; supplemental Figure 2A). These data suggest that BM T_{TE} cells

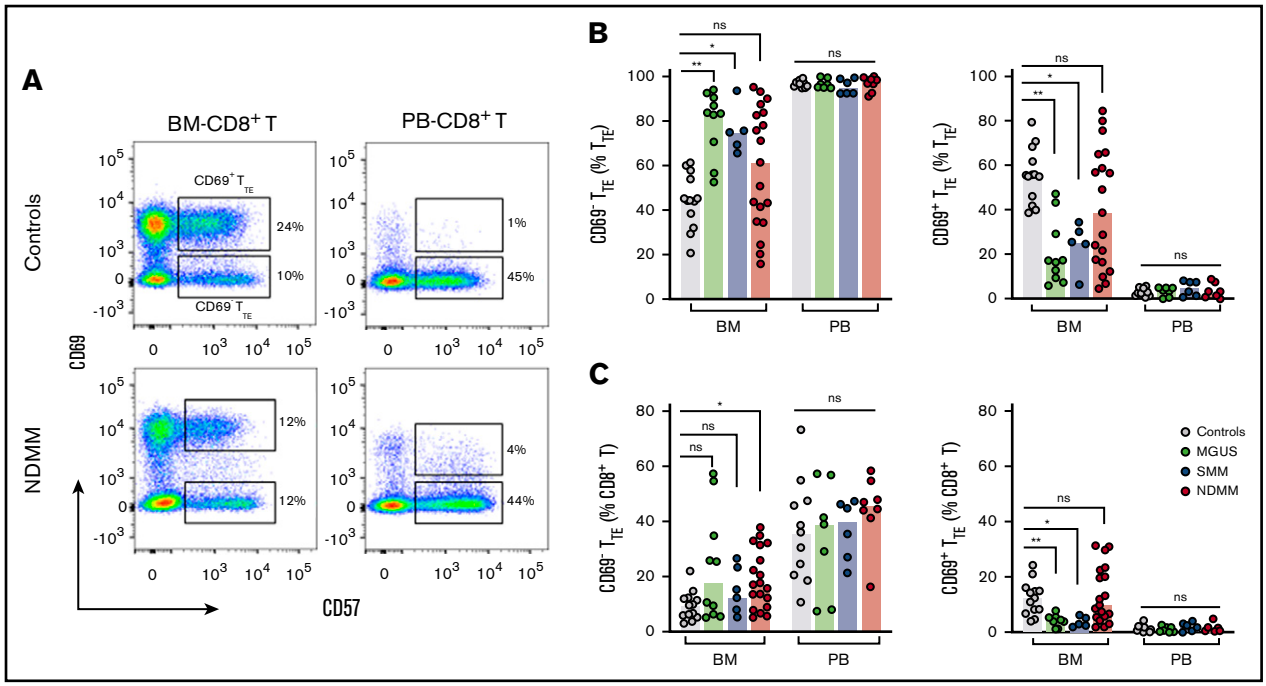

Figure 1. Tissue distribution of CD69$^-$T$_{TE}$ and CD69$^+$ T$_{TE}$ cells in controls and MGUS, SMM, and NDMM patients. (A) Representative dot plots gated for CD8$^+$ T cells show distribution of CD69$^+$T$_{TE}$ and CD69$^-$T$_{TE}$ cells in the BM and PB of controls and NDMM patients. Regions occupied by CD69$^+$T$_{TE}$ and CD69$^-$T$_{TE}$ cells are indicated. Numbers indicate proportions of CD69$^+$T$_{TE}$ and CD69$^-$T$_{TE}$ cells within BM-CD8$^+$T and PB-CD8$^+$T cells. Bars (median with scatter plots) show proportions of CD69$^-$T$_{TE}$ and CD69$^+$T$_{TE}$ cells within T$_{TE}$ (B) and CD8$^+$T (C) cells in the BM of controls (n = 13), MGUS patients (n = 10), SMM patients (n = 5), and NDMM patients (n = 19) and PB of controls (n = 13), MGUS patients (n = 7), SMM patients (n = 6), and NDMM patients (n = 8). *$P < .05$; **$P < .01$; Kruskal-Wallis test with Dunn's multiple comparisons. ns, not significant.

possess inherent non–myeloma-related heterogeneity (based on CD69 expression) that is differently regulated during progression from MGUS and/or SMM to NDMM and that there is an accumulation of both CD69$^-$T$_{TE}$ and total T$_{TE}$ cells (expressed as a percentage of CD8$^+$T cells) in the BM of NDMM patients.

Inverse relationship between CD69$^-$T$_{TE}$ and CD69$^+$T$_{TE}$ cells in BM of NDMM patients, but not in MGUS patients and controls

We next analyzed whether the different contribution of CD69$^-$ and CD69$^+$ subsets to BM-T$_{TE}$ compartments of controls and MGUS and NDMM patients along with the increase in CD69$^-$T$_{TE}$ and total T$_{TE}$ cells seen in BM of NDMM patients involve different relationships between various memory/effector subsets within CD8$^+$ T cells. We analyzed relationships between CD69$^-$T$_{TE}$ cells, CD69$^+$T$_{TE}$ cells, total T$_{TE}$ cells, conventional T memory cells (CD8$^+$CD57$^-$CD45RO$^+$T$_M$), and total CD8$^+$T cells (Figure 2; supplemental Figure 3). SMM patients were excluded from this analysis due to limited numbers (SMM, n = 5, Figure 1B-C; supplemental Figure 2A). In controls, there was a positive correlation between CD69$^-$ and CD69$^+$ subsets within the BM-T$_{TE}$ compartment. Further, there was a strong positive correlation between total BM-T$_{TE}$ cells and their CD69$^-$ and CD69$^+$ subsets (Figure 2A,D-E). Compared with controls, MGUS patients maintained only a strong positive correlation between total BM-T$_{TE}$ cells and their CD69$^-$ subset (Figure 2B,D-E). None of the positive correlations observed in controls and MGUS patients were sustained in NDMM patients; instead, a negative correlation was established between CD69$^-$ and CD69$^+$ subsets within the BM-T$_{TE}$ compartment (Figure 2C-E). These data suggest that inverse relationships established between CD69$^-$ and CD69$^+$ subsets within the BM-T$_{TE}$ compartment discriminate NDMM from MGUS and controls.

Oligoclonal expanded CD69$^-$T$_{TE}$ cells contain myeloma-reactive cells capable of eliminating autologous CD38^{hi}PCs

Our group has previously reported the presence of oligoclonal expansions expressing different TCR-Vβ families within PB-CD8$^+$ T cells in the majority of MM patients.[7] To reveal oligoclonal expansions within CD8$^+$T$_{TE}$ cells that may be overlooked at the level of CD8$^+$T cells, we assessed TCR-Vβ usage within PB T$_{TE}$ cells in age-matched controls and patients with MGUS, SMM, and NDMM (Figure 3A). As expected based on the known oligoclonality of T$_{TE}$ cells,[24] TCR-Vβ expansions were evident in 98.8% (84 out of 85) of analyzed samples, with an average of 3 expanded TCR-Vβ families detected per sample. The average size of the oligoclonal expansions expressed as a percentage of PB-T$_{TE}$ cells was higher in NDMM (12.2%) than in controls (10.3%), MGUS (8.7%), and SMM (8.6%) (Figure 3A). Although the data may be skewed due to differences in the numbers of subjects in each group, results suggest that expanded TCR-Vβ families account for higher proportions of PB T$_{TE}$ in NDMM than in MGUS (Figure 3A). Since the significance of oligoclonal expansions comprising <5% of PB-T$_{TE}$ cells maybe not conclusive, we excluded them from further analysis. The percentage of oligoclonal expansions of size >5% of

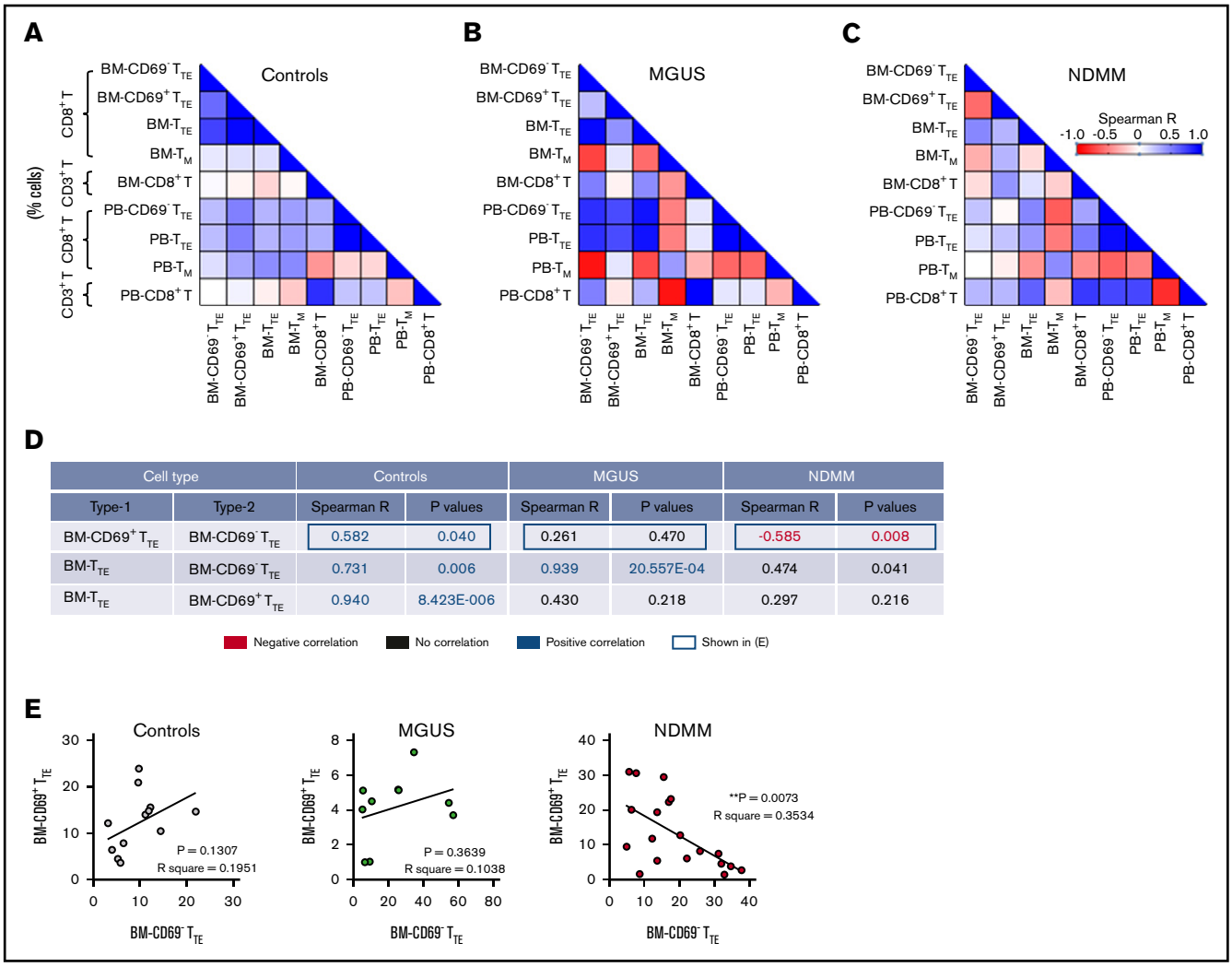

Cell type		Controls		MGUS		NDMM	
Type-1	Type-2	Spearman R	P values	Spearman R	P values	Spearman R	P values
BM-CD69+ T_{TE}	BM-CD69- T_{TE}	0.582	0.040	0.261	0.470	-0.585	0.008
BM-T_{TE}	BM-CD69- T_{TE}	0.731	0.006	0.939	20.557E-04	0.474	0.041
BM-T_{TE}	BM-CD69+ T_{TE}	0.940	8.423E-006	0.430	0.218	0.297	0.216

Negative correlation | No correlation | Positive correlation | Shown in (E)

Figure 2. Relationships between proportions of CD69$^-$$T_{TE}$, CD69$^+$ T_{TE}, T_{TE}, T_M, and CD8$^+$T cells in controls and MGUS and NDMM patients. (A-B) The matrix shows correlations between proportions of CD69$^-$$T_{TE}$, CD69$^+$$T_{TE}$, T_{TE}, T_M (CD8$^+$CD45RO$^+$CD57$^-$), and CD8$^+$T cells in the BM and PB of controls (A), MGUS patients (B), and NDMM patients (C). Proportions of CD69$^-$$T_{TE}$, CD69$^+$$T_{TE}$, T_{TE} and T_M are presented as % CD8$^+$T cells and proportion of CD8$^+$T as % CD3$^+$T cells. (D) The table shows selected significant negative (in red) and positive (in blue) correlations depicted from panels A-C with Spearman $R < -0.5$ and > 0.5 and $P < .05$. (E) Relationships between paired proportion of CD69$^+$$T_{TE}$ and CD69$^-$$T_{TE}$ cells in BM of controls (left), MGUS patients (middle), and NDMM patients (right) analyzed by linear regression model. $^{**}P < .01$.

PB T_{TE} cells was higher in NDMM (83.7%) than in controls (74.7%), MGUS (76.9%), or SMM (76.3%) (supplemental Figure 4). Occasionally, very highly expanded TCR-Vβ families representing >50% of PB T_{TE} cells were detected across cohorts (Figure 3A; supplemental Figure 4). In addition, the majority of expanded TCR-Vβ families were shared between BM-T_{TE} and PB-T_{TE} cells of NDMM patients (Figure 3B).

The increase in the percentage of oligoclonal expanded TCR-Vβ families within PB-T_{TE} of NDMM suggested intensified immune responses. To address the possibility that these responses may be mediated by PB-T_{TE} cells against the patient's myeloma, we purified oligoclonal expanded PB-T_{TE} cells expressing the dominant TCR-Vβ family from the remaining PB-T_{TE} cells within that individual and tested both populations for their capacity to kill autologous CD38^{hi} PCs in a 2-hour culture assay (Figure 3C-D). Contamination by natural killer T (NKT) cells (CD3$^+$CD56$^+$CD16$^+$ cells) and γδ T cells was negligible, as NKT cells represented <5% and γδ T cells were undetectable in PB-T_{TE} compartment (data not shown). PB-T_{TE} cells expressing the dominant TCR-Vβ families eliminated on average 70% of autologous CD38^{hi}PCs within the last hour of a 2-hour culture assay (Figure 3D). Elimination of CD38^{hi}PCs involved caspase-3 activation; however, we were not able to demonstrate an increase in caspase-3 activity in CD38^{hi}PCs cultured with oligoclonal expanded PB-T_{TE} (either at 1- or 2-hour time points), likely due to the rapid cell death following caspase-3 activation (data not shown). In 8 out of 9 patients, oligoclonal expanded PB-T_{TE} cells expressing the dominant TCR-Vβ family were superior to the remaining PB-T_{TE} cells in eliminating autologous CD38^{hi}PCs (Figure 3D). However, PB-T_{TE} cells that did not contain the dominant oligoclonal expansion also exhibited some cytotoxic activity against autologous CD38^{hi}PCs (eliminating on average

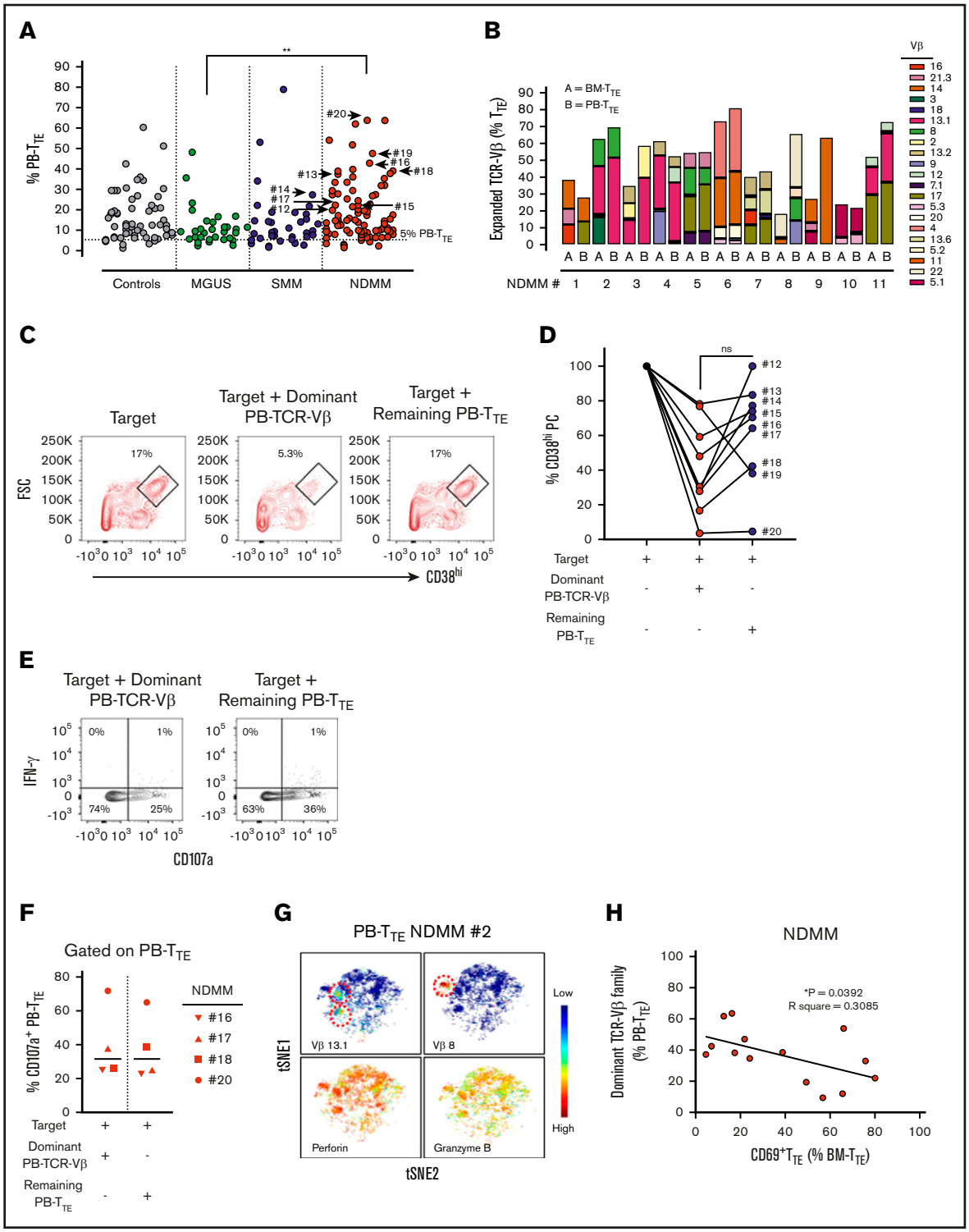

Figure 3. Distribution and function of oligoclonal expanded PB T_{TE} cells. (A) Scatter plots of oligoclonal expansion of TCR-Vβ family–expressing populations within PB-T_{TE} cells of controls (n = 26), MGUS patients (n = 13), SMM patients (n = 10), and NDMM patients (n = 36). Expanded TCR-Vβ family–expressing populations were defined when the percentage of T_{TE} cells expressing that TCR-Vβ family was >3 SD higher than the mean frequency within $CD8^+T_N$ compartment of healthy blood donors (see "Materials and methods"). Each dot represents the percentage of PB-T_{TE} cells with an individual TCR-Vβ family expansion, with multiple expansions shown for each subject (average 3 expanded TCR-Vβ families per subject). The arrows indicate selected dominant TCR-Vβ family expansions that were tested for capacity to kill autologous $CD38^{hi}$PCs (n = 9; #12 to #20; see below, panel D). (B) Oligoclonal expansion of TCR-Vβ family–expressing populations in paired BM-T_{TE} and PB-T_{TE} of NDMM patients (n = 11, #1 to #11). Each colored segment in a stacked vertical bar indicates the proportion of an individual oligoclonal expansion within total BM-T_{TE} and PB-T_{TE} compartment. (C) Dot plots gated for $CD3^-CD14^-$ cells show $CD38^{hi}$PCs after a 2-hour culture assay with the target ($CD3^+$T-cell-depleted BM MNCs) alone, the target with flow-sorted

30% of autologous CD38^{hi}PCs), suggesting that smaller oligoclonal expansions also contribute to antimyeloma activity (Figure 3D). At the 2-hour time point of coculture, both PB-T_{TE} cells expressing the dominant TCR-Vβ family and the remaining PB-T_{TE} cells exhibited comparable levels of degranulation, as measured by CD107a expression, without concordant IFN-γ production (Figure 3E-F). These results indicate that the enhanced cytotoxic capacity of PB-T_{TE} cells expressing the dominant TCR-Vβ family against autologous CD38^{hi}PCs likely relies on increased perforin and granzyme B content (Figure 3G) rather than on increased activity of degranulation. This is the first direct evidence supporting autologous antimyeloma responses mediated by oligoclonal expanded PB-T_{TE} cells. It is worth noting that myeloma-reactive PB-T_{TE} cells expressing the dominant TCR-Vβ family inversely correlate with CD69$^+$$T_{TE}$ (Figure 3H), implying that antimyeloma responses may be limited in NDMM patients with increased proportions of CD69$^+$ T_{TE} cells in their BM.

Phenotypic and functional differences between CD69$^-$$T_{TE}$ and CD69$^+$$T_{TE}$ cells revealed by mass cytometry

We used mass cytometry[18] and FlowSOM clustering analyses[19] to obtain a more comprehensive signature of CD69$^-$$T_{TE}$ and CD69$^+$ T_{TE} cells in NDMM. In agreement with flow cytometry data, we confirmed the presence and tissue distribution of CD69$^-$$T_{TE}$ and CD69$^+$$T_{TE}$ cells in NDMM (Figure 4A). By including mAbs to detect dominant oligoclonal expansions in matched PB and BM samples, we demonstrated that oligoclonal expanded T_{TE} cells were restricted to the CD69$^-$$T_{TE}$ subset in BM and PB of NDMM patients (Figure 4B-C). This suggests that BM-CD69$^-$$T_{TE}$ cells could be the direct counterpart of the PB-CD69$^-$$T_{TE}$ cells capable of killing autologous CD38^{hi}PCs in vitro.

To further define the phenotype of CD69$^-$$T_{TE}$ and CD69$^+$$T_{TE}$ cells, we examined the expression of additional molecules within the CD69$^+$$T_{TE}$ and oligoclonal expanded CD69$^-$$T_{TE}$ cells expressing the dominant TCR-Vβ family in PB and BM of NDMM patients. BM-CD69$^+$$T_{TE}$ cells expressed a Tbet^{lo}Eomes^{hi} transcriptional signature and low perforin and granzyme B (Figure 4D-E). In contrast, the phenotype of BM-CD69$^-$$T_{TE}$ cells strongly indicated cytotoxic function, with high expression of perforin and granzyme B and the reciprocal Tbet^{hi}Eomes$^{lo/neg}$ signature (Figure 4D-E). The dominant TCR-Vβ13.1$^+$ oligoclonal expansion within BM-CD69$^-$$T_{TE}$ and PB-CD69$^-$$T_{TE}$ cells shared the cytotoxic phenotype and transcriptional signature of the CD69$^-$$T_{TE}$ population as a whole (Figure 4E). Both BM-CD69$^-$$T_{TE}$ and BM-CD69$^+$$T_{TE}$ cells produced the cytokines IFN-γ and TNF-α at equivalent levels (Figure 4F). BM-CD69$^+$$T_{TE}$ were further distinguished from oligoclonal expanded CD69$^-$$T_{TE}$ expressing the dominant TCR-Vβ family in PB and BM of NDMM by decreased expression of CD45RA, retention of CD27 and CD28, and higher expression of several inhibitory checkpoints, CD279 (PD-1), TIGIT, CD223 (Lag3), and CD160 (supplemental Figure 5). Overall, based on the expression of CD69, BM residency, cytokine production, and inhibitory checkpoint expression, CD69$^+$$T_{TE}$ cells appear closely related to T_{RM} cells,[23] while the phenotype of the oligoclonal expanded CD69$^-$$T_{TE}$ cells was that of highly cytotoxic CD8$^+$$T_{TE}$ cells.

CD69$^+$$T_{TE}$ cells account for a small proportion of T_{TE} cells in BM of MGUS patients

Using mass cytometry, we next compared CD69$^-$$T_{TE}$, CD69$^+$$T_{TE}$, and total T_{TE} cells in small cohorts of premalignant MGUS and NDMM patients, aiming to understand CD69$^-$$T_{TE}$-cell and CD69$^+$ T_{TE}-cell development during disease progression. We used 2 approaches: manual gating and FlowSOM clustering of mass cytometry data. Although data are preliminary (due to limited availability of BM samples from MGUS patients), both CD69$^-$$T_{TE}$ and CD69$^+$$T_{TE}$ cells were clearly identified within total BM-T_{TE} cells in MGUS and maintain the same tissue distribution as their counterparts in NDMM (Figure 5A-C). CD69$^+$$T_{TE}$ and total T_{TE} cells accounted for a significantly lower proportion of BM-CD8$^+$ T cells in MGUS than in NDMM (Figure 5D; supplemental Figure 2B). In particular, CD69$^+$$T_{TE}$ cells were very sparse, representing on average 13.8% of T_{TE} cells and 2.1% of CD8$^+$ T cells in BM of MGUS patients (Figure 5C-D). Expression of CD69 on T_M cells, and the extent of its downregulation during the transition from the T_M to the T_{TE} stage of differentiation, appeared to be related to the proportions of CD69$^+$$T_{TE}$ cells in BM of NDMM and MGUS patients (Figure 5E). Our data suggest that CD69 expression may be amplified on T_M and T_{TE} cells in BM of NDMM compared with their counterparts in BM of MGUS patients.

Finally, to compare the degree of heterogeneity of BM-T_{TE} cells in both MGUS and NDMM, we analyzed the phenotypes of the 25 metaclusters (MCs) generated by FlowSOM clustering (Figure 5F-G). This revealed that BM-CD69$^+$$T_{TE}$ cells, like their CD69$^-$$T_{TE}$ counterparts, are still phenotypically heterogeneous in both MGUS and NDMM. CD69$^+$$T_{TE}$ can be subdivided into 4 MCs based on differences in expression of CD45RA, CD45RO, CD27, CD28, CD279, and CD38 while uniformly expressing TIGIT, KLRG1, and CD49d and lacking expression of CD127, CD197 (CCR7), CD62L, and CD39 (Figure 5F). These 4 MC are variable in size but persist in all MGUS and NDMM patients (Figure 5G).

Discussion

This study provides the first definitive evidence that circulating oligoclonal expanded cytotoxic CD69$^-$$T_{TE}$ cells are myeloma-reactive cells capable of eliminating autologous CD38^{hi}PCs in vitro.

Figure 3. (continued) autologous oligoclonal expanded PB-T_{TE} cells expressing the subject's dominant TCR-Vβ family, or the target with flow-sorted autologous PB-T_{TE} cells not expressing the dominant TCR-Vβ family (remaining PB-T_{TE} cells). Boxes and numbers indicate the percentage of CD38^{hi}PCs recovered in each culture condition. FSC, forward scatter. (D) Graph shows percentage of CD38^{hi}PCs recovered in culture with PB-T_{TE} cells expressing dominant TCR-Vβ family or with remaining PB-T_{TE} cells, normalized to the percentage of CD38^{hi}PCs recovered in culture with target only. The dominant TCR-Vβ family expansion from each of 9 tested patients (NDMM, #12-13,#15-20; SMM, #14) is indicated by an arrow in Figure 3A. (E) Dot plots show cell surface CD107a and intracellular IFN-γ expression. (F) Graph shows proportions of CD107a$^+$$T_{TE}$ cells (n = 4) in PB-T_{TE} cells expressing dominant TCR-Vβ family and remaining PB-T_{TE} cells after a 2-hour culture assay with target. (G) tSNE plots show distribution of Vβ13.1 and Vβ8 family–expressing PB-T_{TE} cells (top, indicated by red dotted circles) with high perforin and granzyme B expression (bottom) within PB-T_{TE} cells of NDMM #2. (H) Relationship between paired proportion of PB-T_{TE} cells expressing dominant TCR-Vβ family (presented as percentage of PB-T_{TE} cells) and CD69$^+$$T_{TE}$ cells (presented as percentage of BM-T_{TE} cells) in NDMM patients (n = 14) analyzed by linear regression model. *$P < .05$; **$P < .01$.

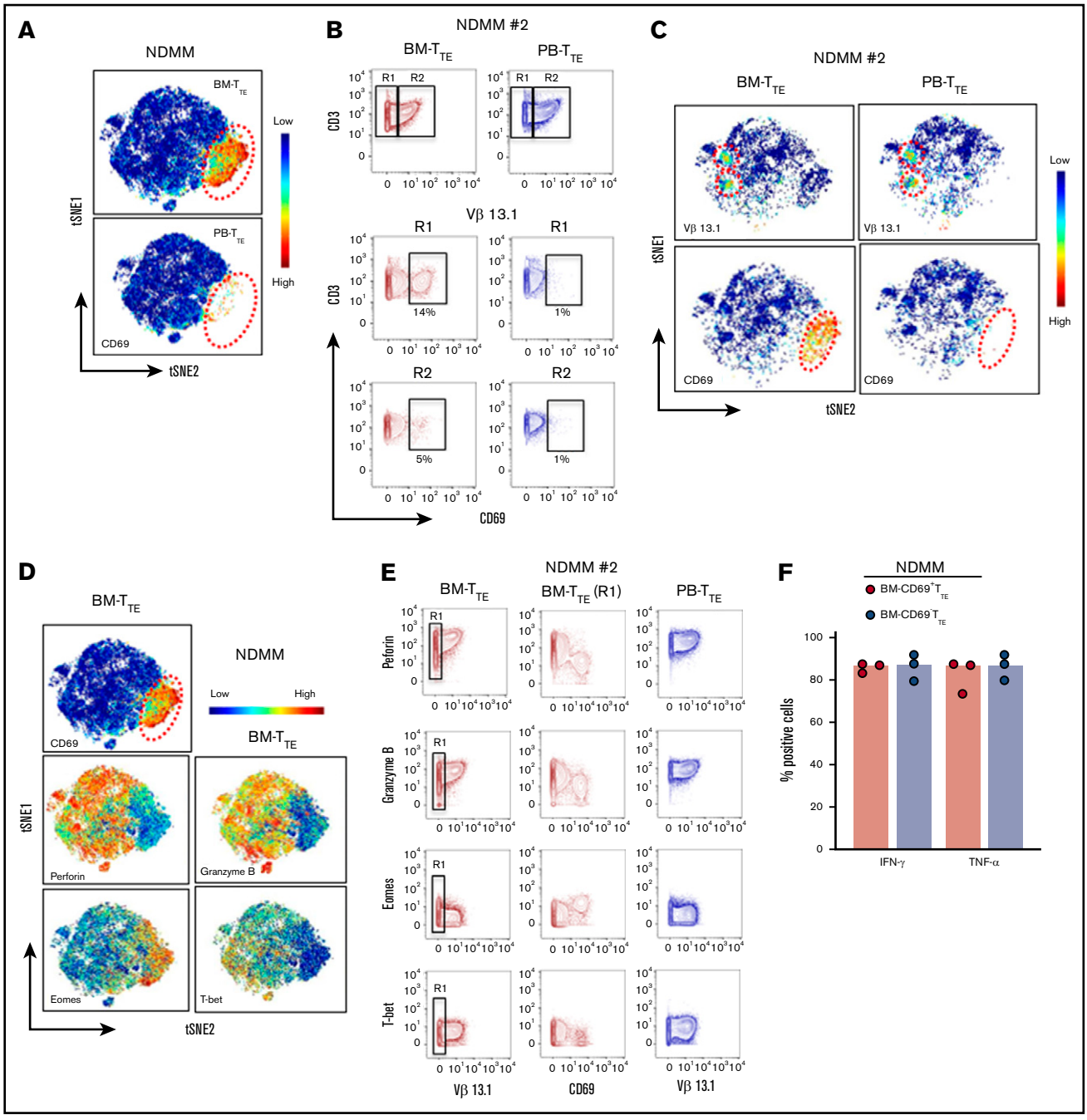

Figure 4. Detailed phenotype of CD69$^-$ T_{TE} and CD69$^+$ T_{TE} cells in NDMM patients. (A-E) Mass cytometry data. (F) Fluorescence flow cytometry data. (B-C,E) Data from 1 representative NDMM patient (NDMM #2; Figure 3B,G). (A) tSNE plots show distribution of CD69$^-$$T_{TE}$ and CD69$^+$$T_{TE}$ cells within pooled BM-T_{TE} and PB-T_{TE} cells of NDMM patients (n = 5). The area occupied by CD69$^+$$T_{TE}$ cells is indicated by the red dotted circle. (B) Biaxial contour plots show BM-T_{TE} and PB-T_{TE} cells containing oligoclonal expanded Vβ13.1 family–expressing cells of NDMM patient #2. Regions indicate Vβ13.1$^-$$T_{TE}$ cells (R1) and Vβ13.1$^+$$T_{TE}$ cells (R2, top panel). Biaxial contour plots gated for Vβ13.1$^-$$T_{TE}$ cells (R1, middle panels) and Vβ13.1$^+$$T_{TE}$ cells (R2, bottom panels) show presence of CD69$^+$$T_{TE}$ cells indicated by boxes and numbers. (C) tSNE plots show distribution of Vβ13.1 family–expressing T_{TE} cells (top) and CD69$^+$$T_{TE}$ cells (bottom) within BM-T_{TE} and PB-T_{TE} cells of NDMM #2 indicated by red dotted circles. (D) tSNE plots show distribution of CD69, perforin, granzyme B, Eomes, and T-bet within pooled BM-T_{TE} cells of NDMM patients (n = 5). (E) Biaxial contour plots showing expression of perforin, granzyme B, Eomes, and T-bet in oligoclonal expanded Vβ13.1 family–expressing cells and remaining T_{TE} cells in BM and PB of NDMM patient #2. Gated BM-T_{TE} cells that do not express Vβ13.1 family (R1) are shown in the middle panels. (F) Bars (median with scatter plots) show proportion of BM-CD69$^+$$T_{TE}$ and BM-CD69$^-$$T_{TE}$ cells producing IFN-γ and TNF-α (NDMM, n = 3).

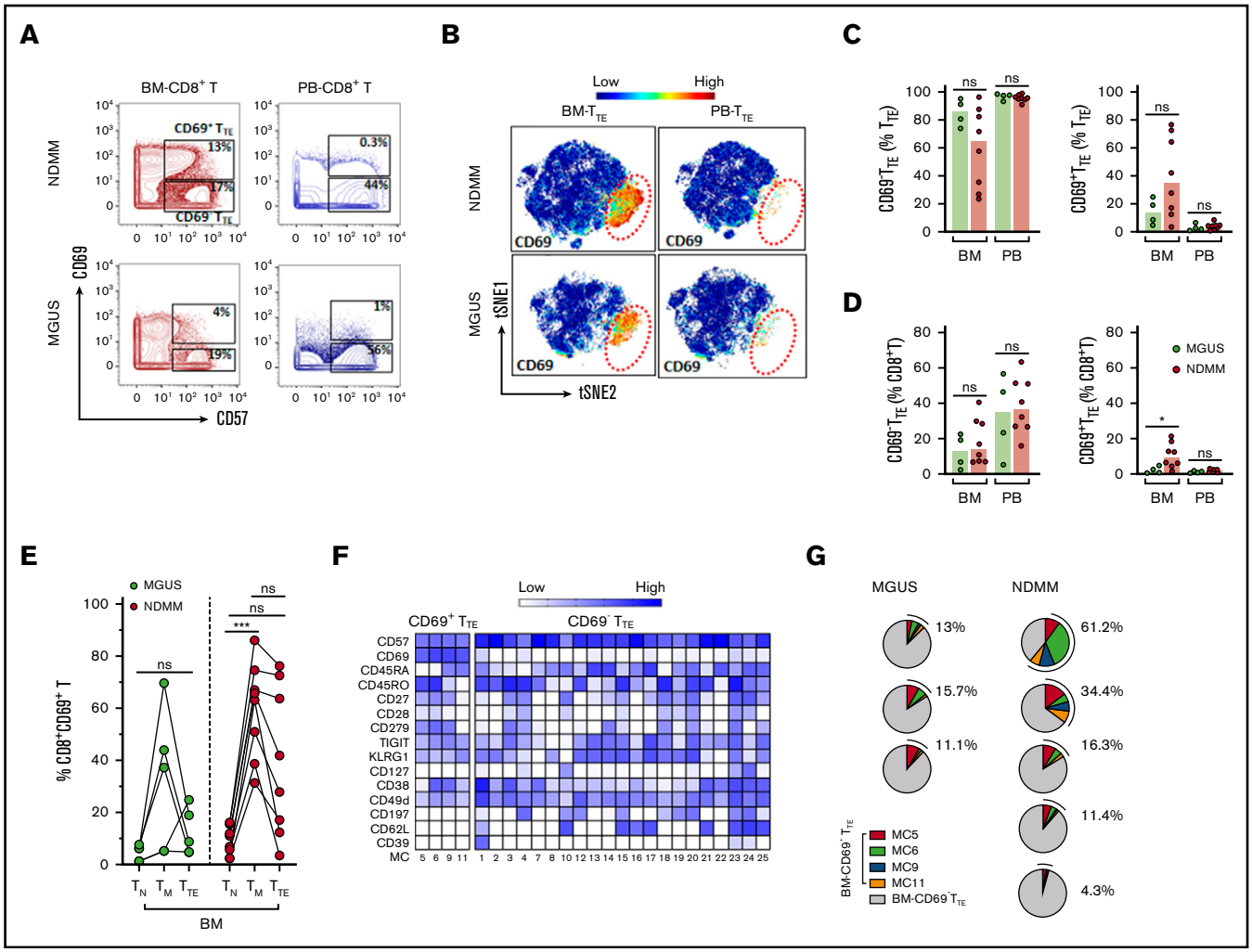

Figure 5. Mass cytometric analysis of T_{TE} cells in MGUS and NDMM patients. (A) Biaxial contour plots gated for $CD8^+$T cells show distribution of $CD69^+T_{TE}$ and $CD69^-T_{TE}$ cells in NDMM and MGUS patients. Regions occupied by $CD69^+T_{TE}$ and $CD69^-T_{TE}$ cells are indicated. Numbers indicate proportions of $CD69^+T_{TE}$ and $CD69^-T_{TE}$ cells within BM-$CD8^+$T and PB-$CD8^+$T cells of NDMM and MGUS patients. (B) tSNE plots show distribution of $CD69^-T_{TE}$ and $CD69^+T_{TE}$ cells within pooled BM-T_{TE} and PB-T_{TE} cells of NDMM patients (n = 5, shown in Figure 4A) and MGUS patients (n = 3). The area occupied by $CD69^+T_{TE}$ cells is indicated by the red dotted circle. Bars (median with scatter plots) show proportions of $CD69^-T_{TE}$ and $CD69^+T_{TE}$ cells within T_{TE} (C) and $CD8^+$T (D) cells in the BM and PB of NDMM (n = 8) and MGUS (n = 4) patients. *$P < .05$. (E) Graph shows proportion of $CD69^+$ cells within the T_N, T_M, and T_{TE} compartments in the BM of MGUS (n = 4) and NDMM (n = 8) patients. T_N, T_M, and T_{TE} cells from the same patient are connected by lines. ***$P < .001$; Friedman test with Dunn's multiple comparators. (F) Heat map showing the phenotype of the 25 MCs defined by FlowSOM analysis of T_{TE} cells. MC5, MC6, MC9, and MC11 contain $CD69^+T_{TE}$ cells, and $CD69^-T_{TE}$ cells are distributed within the remaining 21 MCs. The intensity of the color in each cell indicates the median signal intensity for an individual marker (row) in an individual MC (column). (G) Pie charts show the contribution of $CD69^+T_{TE}$ cells assigned to MC5, MC6, MC9, and MC11 to the BM-T_{TE} cells in NDMM (n = 5) and MGUS (n = 3) patients. Numbers indicate total $CD69^+T_{TE}$ cells within MC5, MC6, MC9, and MC11 in each patient, expressed as a percentage of total BM-T_{TE} cells.

It also suggests the novel concept that balance between cytotoxic oligoclonal expanded $CD69^-T_{TE}$ cells and noncytotoxic $CD69^+T_{TE}$ cells, which resemble T_{RM} cells with BM residency, may regulate immune responses in NDMM patients.

The most clinically important outcome of this study is the demonstration that antimyeloma responses occur in NDMM patients and are executed by oligoclonal expanded PB-$CD69^-T_{TE}$ cells. Thus, oligoclonal expanded PB-$CD69^-T_{TE}$ cells, which we previously reported as "T-cell clones,"[7] are indeed myeloma reactive. Elimination of autologous $CD38^{hi}$PCs occurs rapidly within a 2-hour culture, likely through degranulation and release of preformed perforin and granzyme from lytic granules of PB-$CD69^-T_{TE}$ cells. As expected, no IFN-γ production was detected after 2 hours of culture, as it requires a longer time to be produced de novo following T-cell activation.[25] The potent cytotoxic functions of myeloma-reactive PB-$CD69^-T_{TE}$ cells are further reinforced by their lower expression of inhibitory receptors, CD279, TIGIT, Lag 3, and CD160, consistent with our previous studies.[11,26] Mass cytometric analysis indicated a high degree of similarity between $CD69^-T_{TE}$ cells in PB and BM, and this similarity is further extended to the dominant oligoclonal expansions present in both tissues (BM and PB) of NDMM patients. Direct testing of oligoclonal expanded $CD69^-T_{TE}$ cells in the BM for their myeloma reactivity remains

challenging due to their limited numbers and small volume of diagnostic BM samples available for research. However, our data are consistent with the concept that myeloma-reactive cells likely arise within MIL in the MM microenvironment and undergo oligoclonal expansion and terminal differentiation into CD69^{-}T$_{TE}$ cells, which then circulate between BM and PB.

We found that myeloma reactivity is not restricted to oligoclonal expanded PB-CD69^{-}T$_{TE}$ cells expressing dominant TCR-Vβ families, since remaining PB-CD69^{-}T$_{TE}$ cells expressing less expanded TCR-Vβ families also retain some capacity to eliminate autologous CD38^{hi}PCs. Also, highly expanded TCR-Vβ families representing >50% of PB-T$_{TE}$ cells are not restricted to patients, as they are occasionally seen in age-matched controls, perhaps induced by aging-associated autoimmune and infective processes.[27] We ruled out the possibility that contaminating NKT and γδ T cells play a significant role in the elimination of autologous CD38^{hi}PCs. This is consistent with the observation that NKT and γδ T cells are not required for antimyeloma immunity in mice bearing Vk*MYC myeloma and that CD8^{+}T-cell clones of rare, small, and medium size are protective.[1] Nonetheless, antigen specificity of readily accessible TCR-Vβ restricted myeloma-reactive PB-CD69^{-}T$_{TE}$ cells could be further explored, in particular by testing for restriction to major histocompatibility complex class I–related molecule (MR1), which is expressed on myeloma cells.[28] The possibility that PB-CD69^{-}T$_{TE}$ cells include MR1-reactive T cells capable of killing a variety of cancers expressing MR1[29,30] is an interesting future research topic.

Our finding that oligoclonal expanded PB-CD69^{-}T$_{TE}$ cells in NDMM patients are highly functional conflicts with a number of reports that T cells in MM patients are dysfunctional, senescent, and/or exhausted.[13,14,16] Our data strongly support the concept that potent antimyeloma immunity mediated by oligoclonal expanded CD69^{-}T$_{TE}$ cells persists in NDMM. However, how these naturally induced circulating myeloma-reactive CD69^{-}T$_{TE}$ cells can be retained within MIL and protected from the harmful effects of myeloma therapeutics is not clear. In particular, it will be important to determine the sensitivity of myeloma-reactive CD69^{-}T$_{TE}$ cells to myeloma therapies and to understand their role in the immunological aspects of autologous stem cell transplantation, a front-line therapy for transplant-eligible MM patients.[20]

In addition to defining myeloma-reactive cytotoxic CD69^{-}T$_{TE}$ cells, this study provides a detailed analysis of noncytotoxic, proinflammatory BM-CD69^{+}T$_{TE}$ cells that are present in controls and all patient groups. Correlative analysis performed in this study revealed that noncytotoxic BM CD69^{+}T$_{TE}$ cells maintained inverse relationships with their CD69^{-}T$_{TE}$ counterparts within BM-T$_{TE}$ cells of NDMM patients, but not MGUS patients and controls. They also maintain negative relationships with myeloma-reactive oligoclonal expanded PB-CD69^{-}T$_{TE}$ cells expressing dominant TCR-Vβ families indicating altered immune homeostasis over and above the direct effect of oligoclonal expansion within the CD69^{-}T$_{TE}$ subset. How the development of CD69^{+}T$_{TE}$ and CD69^{-}T$_{TE}$ cells within the BM-T$_{TE}$ compartment is regulated remains unclear. However, our mass cytometry data suggest that the development of BM-CD69^{+}T$_{TE}$ cells may be more closely related to the transition from T$_{M}$ cells expressing CD69 rather than from CD69^{-}T$_{TE}$ cells and that regulation of this transition may differ between NDMM and MGUS patients.

We demonstrated that CD69^{+}T$_{TE}$ cells have markedly different properties from cytotoxic CD69^{-}T$_{TE}$ cells, including low expression of the cytotoxic molecules perforin and granzyme B, an Eomes^{hi} Tbet$^{low/neg}$ transcriptional signature, and high expression of multiple inhibitory checkpoints, such as CD279, TIGIT, Lag 3, and CD160, suggesting CD69^{+}T$_{TE}$ cells may be a suitable target for checkpoint inhibition immunotherapy.[17] CD69^{+}T$_{TE}$ cells reside in the BM and appear closely related to T$_{RM}$ cells.[23] Small proportions of CD8^{+} CD69^{+}CD57^{+}T$_{RM}$ cells have been reported in human lung and spleen[23] and may be equivalent to the CD69^{+}T$_{TE}$ cells described in this study. To the best of our knowledge, this is the first documentation of BM-resident CD69^{+}T$_{TE}$ cells, which likely belong to the resident CD8^{+}CD69^{+} cells seen in human BM.[31]

We found that CD69^{+}T$_{TE}$ cells account for highly variable proportions of the BM-T$_{TE}$ compartment in NDMM patients (5% to 84%), a finding that may relate to clinical heterogeneity. CD69^{+} T$_{TE}$ cells appear to be less frequent within BM-T$_{TE}$ cells of MGUS and SMM patients (6% to 47% MGUS; 6% to 34% SMM), suggesting that progression to clinical MM, at least in some patients, may be associated with an accumulation of noncytotoxic CD69^{+}T$_{TE}$ cells within MILs. Accumulation of CD69^{+}T$_{TE}$ within MILs may contribute to local inflammation through the production of the proinflammatory cytokines IFN-γ and TNF-α, impair the development of cytotoxic CD69^{-}T$_{TE}$ cells, and thus promote myeloma growth. It has already been demonstrated by a study in CD69-knockout mice that CD69 expression on T cells impaired the antitumor immune response, suggesting CD69 is an attractive target for cancer immunotherapy.[32] Understanding the role of CD69^{+}T$_{TE}$ cells within MILs throughout disease progression has the potential to lead to the development of novel immune-based approaches for the management of MM.

Our study suggests that changes in T$_{TE}$ cells contributing to MILs, without apparent changes in the PB-T$_{TE}$ compartment, are associated with myeloma progression from premalignant MGUS or asymptomatic SMM. Data also suggests that the development of cytotoxic CD69^{-}T$_{TE}$ cells, which mediate antimyeloma responses in NDMM patients, can be affected by the accumulation of noncytotoxic CD69^{+}T$_{TE}$ cells within MILs. Tracing CD69^{+}T$_{TE}$ cells within MILs and correlating their numbers with clinical outcome in MM patients receiving MILs as adoptive T-cell therapy[33,34] could provide essential insights into role of BM-CD69^{+}T$_{TE}$ cells in antimyeloma immunity.

Acknowledgments

The authors thank Alberto Catalano for excellent research management support, RPAH Medical Registrars for collection of patient samples and informed consent, and patients and their families for donating samples for research. They would also like to thank all the support staff at Sydney Cytometry and the Ramaciotti Facility for Human Systems Biology for their assistance with the mass cytometry studies.

This work is funded by a Brian D. Novis research grant from the International Myeloma Foundation (C.E.B.).

Authorship

Contribution: S.V. and C.E.B. designed and performed the research, analyzed the data, and wrote the paper; K.H.A.L. and S.Y. performed the research and analyzed the data; J.F. performed the research, wrote the human ethics, and assisted in writing the paper; H.M.M.

designed and performed mass cytometry assays; G.C. assisted research design and collection of the control samples; B.F.d.S.G. assisted in research design, mass cytometry data analysis, and writing the paper; F.M.-W. assisted with the flow/CAPX approach and analyzed FlowSOM data; N.N. assisted in research design and data analysis; C.E.B., E.A., V.V., D.M., C.B., S.L., S.D., L.K., J.G., and P.J.H. assisted in research design, reviewed patients, and assisted with the collection of patient samples and clinical information; R.B. reviewed patients undergoing hip arthroplasty and designed research; and D.J. and P.J.H. assisted in research design and writing the paper.

Conflict-of-interest disclosure: The authors declare no competing financial interests.

ORCID profiles: S.V., 0000-0002-2803-0717; H.M.M., 0000-0003-2047-6543; B.F.d.S.G., 0000-0001-6817-9690.

Correspondence: Slavica Vuckovic, Royal Prince Alfred Hospital, Level 5, Building 77, Missenden Rd, Camperdown, NSW 2050, Australia; e-mail: slavica.vuckovic@health.nsw.gov.au; and Christian E. Bryant, Royal Prince Alfred Hospital, Level 5, Building 77, Missenden Rd, Camperdown, NSW 2050, Australia; e-mail: christian.bryant@health.nsw.gov.au.

References

1. Vuckovic S, Minnie SA, Smith D, et al. Bone marrow transplantation generates T cell-dependent control of myeloma in mice. *J Clin Invest*. 2019;129(1):106-121.
2. Dong S, Ghobrial IM. Autologous graft versus myeloma: it's not a myth. *J Clin Invest*. 2019;129(1):48-50.
3. Byrne JL, Carter GI, Ellis I, Haynes AP, Russell NH. Autologous GVHD following PBSCT, with evidence for a graft-versus-myeloma effect. *Bone Marrow Transplant*. 1997;20(6):517-520.
4. Tricot G, Vesole DH, Jagannath S, Hilton J, Munshi N, Barlogie B. Graft-versus-myeloma effect: proof of principle. *Blood*. 1996;87(3):1196-1198.
5. Joshua D, Suen H, Brown R, et al. The T cell in myeloma. *Clin Lymphoma Myeloma Leuk*. 2016;16(10):537-542.
6. Perumal D, Imai N, Laganà A, et al. Mutation-derived neoantigen-specific T-cell responses in multiple myeloma. *Clin Cancer Res*. 2020;26(2):450-464.
7. Sze DM, Giesajtis G, Brown RD, et al. Clonal cytotoxic T cells are expanded in myeloma and reside in the CD8(+)CD57(+)CD28(-) compartment. *Blood*. 2001;98(9):2817-2827.
8. Mahnke YD, Brodie TM, Sallusto F, Roederer M, Lugli E. The who's who of T-cell differentiation: human memory T-cell subsets. *Eur J Immunol*. 2013;43(11):2797-2809.
9. Chattopadhyay PK, Betts MR, Price DA, et al. The cytolytic enzymes granyzme A, granzyme B, and perforin: expression patterns, cell distribution, and their relationship to cell maturity and bright CD57 expression. *J Leukoc Biol*. 2009;85(1):88-97.
10. Brown RD, Spencer A, Ho PJ, et al. Prognostically significant cytotoxic T cell clones are stimulated after thalidomide therapy in patients with multiple myeloma. *Leuk Lymphoma*. 2009;50(11):1860-1864.
11. Suen H, Brown R, Yang S, Ho PJ, Gibson J, Joshua D. The failure of immune checkpoint blockade in multiple myeloma with PD-1 inhibitors in a phase 1 study. *Leukemia*. 2015;29(7):1621-1622.
12. Badros A, Hyjek E, Ma N, et al. Pembrolizumab, pomalidomide, and low-dose dexamethasone for relapsed/refractory multiple myeloma. *Blood*. 2017;130(10):1189-1197.
13. Zelle-Rieser C, Thangavadivel S, Biedermann R, et al. T cells in multiple myeloma display features of exhaustion and senescence at the tumor site. *J Hematol Oncol*. 2016;9(1):116.
14. Sponaas AM, Yang R, Rustad EH, et al. PD1 is expressed on exhausted T cells as well as virus specific memory CD8+ T cells in the bone marrow of myeloma patients. *Oncotarget*. 2018;9(62):32024-32035.
15. Bailur JK, McCachren SS, Doxie DB, et al. Early alterations in stem-like/resident T cells, innate and myeloid cells in the bone marrow in preneoplastic gammopathy. *JCI Insight*. 2019;5:5.
16. Kourelis TV, Villasboas JC, Jessen E, et al. Mass cytometry dissects T cell heterogeneity in the immune tumor microenvironment of common dysproteinemias at diagnosis and after first line therapies. *Blood Cancer J*. 2019;9(9):72.
17. Franssen LE, Mutis T, Lokhorst HM, van de Donk NWCJ. Immunotherapy in myeloma: how far have we come? *Ther Adv Hematol*. 2019;10:2040620718822660.
18. Bendall SC, Nolan GP, Roederer M, Chattopadhyay PK. A deep profiler's guide to cytometry. *Trends Immunol*. 2012;33(7):323-332.
19. Van Gassen S, Callebaut B, Van Helden MJ, et al. FlowSOM: using self-organizing maps for visualization and interpretation of cytometry data. *Cytometry A*. 2015;87(7):636-645.
20. Rajkumar SV, Dimopoulos MA, Palumbo A, et al. International Myeloma Working Group updated criteria for the diagnosis of multiple myeloma. *Lancet Oncol*. 2014;15(12):e538-e548.
21. Laurens van der Matten HG. Visualizing data using t-SNE. *J Mach Learn Res*. 2008;9:2579-2605.
22. Ashhurst TM, Cox DA, Smith AL, King NJC. Analysis of the murine bone marrow hematopoietic system using mass and flow cytometry. *Methods Mol Biol*. 2019;1989:159-192.
23. Kumar BV, Ma W, Miron M, et al. Human tissue-resident memory T cells are defined by core transcriptional and functional signatures in lymphoid and mucosal sites. *Cell Rep*. 2017;20(12):2921-2934.

24. Dolstra H, Preijers F, Van de Wiel-van Kemenade E, Schattenberg A, Galama J, de Witte T. Expansion of CD8+CD57+ T cells after allogeneic BMT is related with a low incidence of relapse and with cytomegalovirus infection. *Br J Haematol*. 1995;90(2):300-307.

25. Betts MR, Brenchley JM, Price DA, et al. Sensitive and viable identification of antigen-specific CD8+ T cells by a flow cytometric assay for degranulation. *J Immunol Methods*. 2003;281(1-2):65-78.

26. Suen H, Brown R, Yang S, et al. Multiple myeloma causes clonal T-cell immunosenescence: identification of potential novel targets for promoting tumour immunity and implications for checkpoint blockade. *Leukemia*. 2016;30(8):1716-1724.

27. Strioga M, Pasukoniene V, Characiejus D. CD8+ CD28- and CD8+ CD57+ T cells and their role in health and disease. *Immunology*. 2011;134(1):17-32.

28. Gherardin NA, Loh L, Admojo L, et al. Enumeration, functional responses and cytotoxic capacity of MAIT cells in newly diagnosed and relapsed multiple myeloma. *Sci Rep*. 2018;8(1):4159.

29. Lepore M, Kalinichenko A, Calogero S, et al. Functionally diverse human T cells recognize non-microbial antigens presented by MR1. *eLife*. 2017;6:e24476.

30. Crowther MD, Dolton G, Legut M, et al. Genome-wide CRISPR-Cas9 screening reveals ubiquitous T cell cancer targeting via the monomorphic MHC class I-related protein MR1 [published correction appears in *Nat Immunol*. 21:695]. *Nat Immunol*. 2020;21(2):178-185.

31. Pascutti MF, Geerman S, Collins N, et al. Peripheral and systemic antigens elicit an expandable pool of resident memory CD8$^+$ T cells in the bone marrow. *Eur J Immunol*. 2019;49(6):853-872.

32. Mita Y, Kimura MY, Hayashizaki K, et al. Crucial role of CD69 in anti-tumor immunity through regulating the exhaustion of tumor-infiltrating T cells. *Int Immunol*. 2018;30(12):559-567.

33. Noonan K, Matsui W, Serafini P, et al. Activated marrow-infiltrating lymphocytes effectively target plasma cells and their clonogenic precursors. *Cancer Res*. 2005;65(5):2026-2034.

34. Noonan KA, Huff CA, Davis J, et al. Adoptive transfer of activated marrow-infiltrating lymphocytes induces measurable antitumor immunity in the bone marrow in multiple myeloma. *Sci Transl Med*. 2015;7(288):288ra78.